Liquid Crystals
Publication details, including instructions for authors and subscription information:
http://www.informaworld.com/smpp/title~content=t713926090

On the simulation of the director field of a nematic liquid crystal

A. Kilian[a]; S. Hess[a]
[a] Institut für Theoretische Physik, Technische Universität Berlin, Berlin 12, F.R. Germany

To cite this Article Kilian, A. and Hess, S.(1990) 'On the simulation of the director field of a nematic liquid crystal', Liquid Crystals, 8: 4, 465 — 472
To link to this Article: DOI: 10.1080/02678299008047362
URL: http://dx.doi.org/10.1080/02678299008047362

LIQUID CRYSTALS, 1990, VOL. 8, NO. 4, 465–472

On the simulation of the director field of a nematic liquid crystal

by A. KILIAN and S. HESS
Institut für Theoretische Physik, Technische Universität Berlin, D-1000 Berlin 12, F.R. Germany

(*Received 26 July 1989; accepted 28 April 1990*)

A numerical method for the analysis of the static and dynamic behaviour of the director field, **n**, of a nematic liquid crystal is presented, where the equivalence of **n** and $-\mathbf{n}$ is taken into account. The occurrence of defects characteristic of nematics is studied for a hybrid cell, and for a material with a negative anisotropic susceptibility subject to an external field. Typical director configurations with defects are displayed graphically for some two dimensional arrangements and, in addition, the resulting pictures corresponding to an observation between crossed polarizer and analyser have been computed.

1. Introduction

The local orientation of a nematic liquid crystal is described by the director field **n** [1–3]. As early as 1904, Lehmann [4] concluded from optical observations under the polarization microscope, that certain features in the schlieren texture can be explained by disclinations of the orientation field with half integer winding numbers (half convergence and half core points, [3]) which, in turn, implies that **n** and $-\mathbf{n}$ are physically equivalent. Numerical simulations of the local orientation, and the resulting optical properties of nematics, should be consistent with this fact. Accordingly, this paper presents a numerical method for the analysis of the static and the dynamic behaviour of the director field of a nematic where the physical equivalence of **n** and $-\mathbf{n}$ is taken into account. We have found that the vectorial calculus, well-tried in analytical calculations for decades, proved to be unsatisfactory for simulations in two and three dimensions, because it yields ambiguous solutions due to the polarity of the boundary vectors. We developed, therefore, a tensorial algorithm to overcome these difficulties. A significant result is that our new method leads to some solutions completely different to those achieved with the conventional vectorial calculus. Specifically, it yields the well-known disclination defects, with half-integer winding numbers, to which nematic threads are attached [1, 2]. This implies the ability to simulate physical situations where the director field changes between different stable states which are topologically not equivalent, cf. [5]. Even for one dimensional problems, where the choice of the polarity of the boundary vectors according to the physical problem is trivial, the method has the advantage to make the right choice automatically [16].

Two simple applications of the tensorial simulation method are treated. First, we simulate the behaviour of a hybrid cell, a cell with a homeotropic boundary condition at one wall and planar anchoring at the other. Secondly we simulate a two dimensional nematic liquid crystal with its easy axis and an applied field both in the same direction, but with a negative anisotropic part of the dielectric permeability. This latter example also demonstrates the dynamic properties of the simulation: if the time

0267-8292/90 $3.00

taken for the applied field to reach a maximum value is long compared to the relaxation time of the fluid (which is essentially given by the size of the cell and the Leslie coefficient γ_1, the rotational viscosity [1–3]), the director field retains a uniform configuration. If the maximum field is reached instantaneously, the director field has no time for homogeneous alignment, but clusters with nematic defects can be frozen in. More precisely, if the time for the field to reach its maximum, τ_{ext}, is small compared to the relaxation time of the nematic, τ_{relax}. Contrast pictures of the simulated defects are calculated, as they would appear when examined with monochromatic illumination under crossed nicols.

2. Description of the algorithm

The algorithm [6] is based on the equation of change for the director field $n_\mu(\mathbf{r}, t)$ in an electric field $\mathbf{E}$,

$$\gamma_1 \frac{\partial}{\partial t} n_\mu n_\nu = K\Delta n_\mu n_\nu + \varepsilon_a \varepsilon_0 \overleftrightarrow{E_\mu E_\nu} \tag{1}$$

with the constraint $n_\mu n_\mu$ = constant. Here, γ_1 is the Leslie coefficient, K the Frank elasticity coefficient, and ε_a is the difference $\varepsilon_\parallel - \varepsilon_\perp$ between the relative dielectric coefficients parallel and perpendicular to the applied field at the given temperature. The symbol $\overleftrightarrow{\ldots}$ refers to the symmetric traceless (irreducible) part of a tensor $\mathbf{t}$, i.e.

$$\overleftrightarrow{t_{\mu\nu}} = \tfrac{1}{2}(t_{\mu\nu} + t_{\nu\mu}) - \tfrac{1}{3} t_{\lambda\lambda}\delta_{\mu\nu}.$$

For a magnetic field $\mathbf{B}$, $\varepsilon_0(\varepsilon_\parallel - \varepsilon_\perp)$ is replaced by $\mu_0^{-1}(\chi_\parallel - \chi_\perp)$, $\chi_\parallel, \chi_\perp$ are the relative magnetic susceptibilities. Note that χ here is defined by $M_\mu = \mu_0^{-1}\chi_{\mu\nu}B_\nu$ rather than by $M_\mu = \chi_{\mu\nu}H_\nu$ [3]. Equation (1) can be obtained from an equation for the alignment tensor [7–9] which in turn was derived from a generalized Fokker–Planck equation [10]. That theoretical approach allows a unified treatment of non-equilibrium phenomena in the isotropic and the nematic phases; the de Gennes theory for pretransitional behaviour [1, 2] and the Ericksen–Leslie theory for nematics are special cases of the unfied theory. Equation (1) is essentially an equation for the alignment tensor $a_{\mu\nu}$ in the one coefficient approximation and for the case of uniaxial alignment (which is provided here), where

$$a_{\mu\nu} = (\tfrac{3}{2})^{1/2} a \overleftrightarrow{n_\mu n_\nu}. \tag{2}$$

Since the order parameter, a, is assumed constant due to the constant temperature [1–3] and the derivatives in equation (1) do not affect the constant trace of $n_\mu n_\nu$, $a_{\mu\nu}$ could be replaced by $n_\mu n_\nu$. Following the usual convention, $n_\mu n_\mu$ is chosen to be 1. Multiplying equation (1) by n_ν would lead to the standard vectorial expression

$$\gamma_1 \frac{\partial n_\mu}{\partial t} = K\Delta n_\mu + \varepsilon_0 \varepsilon_a n_\nu E_\nu E_\mu. \tag{3}$$

In order to recover the full anisotropy of the Frank elasticity, the torque $K\Delta n_\mu$ would have to be altered.

In order to preserve the tensorial symmetry, the discretization of equation (1) has to be performed prior to the projection onto the vectorial state. This is done on a rectangular lattice with mesh size δl with the replacement rules

$$\frac{\partial}{\partial t} n_\mu \to \delta t^{-1}(n_\mu^{new} - n_\mu) \tag{4a}$$

and

$$\frac{\partial^2}{\partial r_1^2} G \to \delta l^{-2}[G(i_1 + 1, i_2, i_3) + G(i_1 - 1, i_2, i_3) - 2G(i_1, i_2, i_3)]; \qquad (4b)$$

these hold within an accuracy of δt^{-2} and δl^{-4}, respectively. n_μ^{new} is the value of n_μ at the next time step $t + \delta t$, and the integers i_1, i_2, i_3 are the coordinates of the lattice points. Discretizing equation (3) with the choice

$$\delta t = \frac{\gamma_1 \delta l^2}{2\, dK} \qquad (5)$$

(d is the dimension of the problem) leads to the iterational algorithm

$$n_\mu^{\text{new}} = \lambda\left\{\langle n_\mu n_\nu\rangle + \frac{\beta}{2d}\hat{E}_\mu \hat{E}_\nu\right\} n_\nu. \qquad (6)$$

The brackets indicate an average over the $2d$ nearest neighbours. The parameter λ is inserted in order to fulfil the constraint $n_\mu n_\mu = 1$; it has to be calculated at every interior lattice point. The quantity β depends on the material parameters and the length scale

$$\beta = \frac{\varepsilon_0 \varepsilon_a \delta l^2}{K} E^2$$

$$= \left(\frac{\pi \delta l}{L}\right)^2 \left(\frac{E}{E_{\text{fred}}}\right)^2. \qquad (7)$$

Here, L is the thickness of the cell in the direction of the applied field, and the Freederickz threshold field [1–3] is given by (in the one coefficient approximation)

$$E_{\text{fred}} = \frac{\pi}{L}\left(\frac{K}{\varepsilon_0 |\varepsilon_a|}\right)^{1/2}. \qquad (8)$$

For nematics with $\beta < 0$, i.e. with a negative anisotropy of the dielectric permeability, $\varepsilon_a < 0$, however, a modification is needed for reasons of numerical stability. More specifically, the negative action of the dielectric permeability on the vector $\hat{E}_\mu \hat{E}_\nu n_\nu$ is substituted by a positive action on the complementary vector ($\varepsilon_a < 0$ implies $-\beta > 0$), which leads to

$$n_\mu^{\text{new}} = \lambda\left\{\langle n_\mu n_\nu\rangle\, n_\nu - \frac{\beta}{2d}(n_\mu - \hat{E}_\mu \hat{E}_\nu n_\nu)\right\}. \qquad (9)$$

Now, the implied time scaling depends on the strength of the external field as

$$\delta t = \frac{\gamma_1 \delta l^2}{2dK - \varepsilon_0 \varepsilon_a E^2 \delta l^2} \qquad (10)$$

which means that strong fields cause an effective slowing down of the iteration.

3. Applications

The applications introduced here demonstrate the main features of the tensorial algorithm, namely (1) the different forms of defects (disclinations) typical for nematics, and (2) the orientational dynamics of the nematic. For simplicity, all simulations were performed in two dimensions on a lattice with 21 × 21 points.

The coupling between orientation and flow is disregarded, and, in a first approach, the elasticity of nematics is treated in the one coefficient approximation [1–3]. The contrast pictures of the director configurations were calculated for optimized contrast. In an experiment this is achieved by a suitable matching condition between wavelength, cell thickness and ε_a. The observed intensity then is proportional to $(n_x n_y)^2$ (the light propagates in the z direction). These numbers were transformed into a grey scale.

3.1. *The hybrid cell*

The cell for the simulations is a hybrid cell, which has a homeotropic boundary condition at one wall and a planar one at the other. The disclinations here were generated by isotropically distributed random vectors of unit length. This is not very realistic in the sense that the equations used here cannot describe a phase transition to the isotropic phase. We think, however, that this type of initial condition describes, approximately, a relaxation after a temperature quench.

This example is meant to demonstrate the different forms of disclinations typical for nematics, that occur mainly in the absence of external fields. In real nematics, disclinations are supposingly initiated by local imperfections, which are not taken into consideration here; our simulations refer to a nematic without any impurities. Therefore, we had to find conditions which favour the occurrence of disclinations.

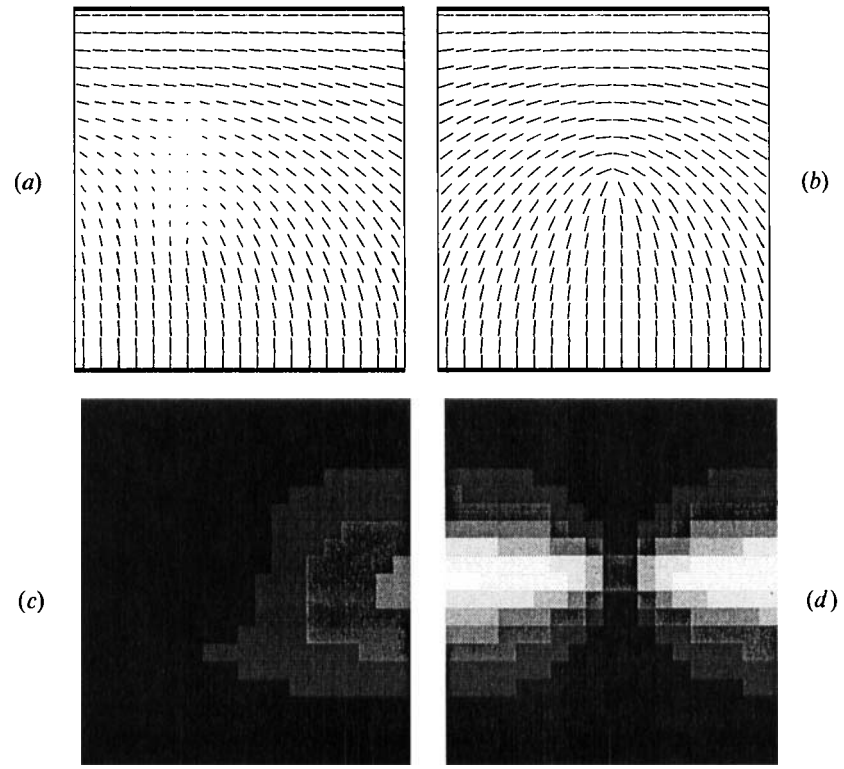

Figure 1. Top: identical boundary conditions can lead to rather different director configurations, which can depend sensitively on the initial conditions. Bottom: the same configurations, seen under crossed nicols.

One method used in former simulations [6] are competing boundary conditions, e.g. a capillary tube with a homeotropic easy axis. Here, the walls are assumed to be on the top and on the bottom of the cell, and the left and the right side were set free (no boundary conditions), which was realised by boundary vectors of zero length. The simulations were repeated several times with different random starting conditions.

The disclinations appearing here are in principle the same as if the simulations were done in three dimensions. To obtain an impression of how they would appear via their birefringence, the intensity of light going through the cell and crossed nicols (in the x and y direction) was calculated. In two dimensions, the direction of incidence has to be perpendicular to the lattice square, the z direction. Thus the cell is homogeneous in the z-direction. Figure 1 shows two stable director configurations, and their contrast pictures. (As an aside, it is impressive that as early as 1904 Lehmann [4] deduced the correct director configurations with the various types of disclinations (cf. his hand sketches reproduced here as figure 4) from similar contrast pictures.) In figure 1(a) there is a region where the director field escapes into the third direction. In the optical picture, this region remains dark when the crossed polarizer and analyser are rotated by 45° (then the transmitted intensity is proportional to $n_x^2 - n_y^2$) whereas in figure 1(d) black areas become white and vice versa. The director field of figure 1(b) contains a half core point. The corresponding optical picture in figure 1(d) shows the typical disclinations with two brushes [2]. In contrast to real nematics, the simulated disclinations did not move during the relaxation, at least not at zero field. Since the flow is neglected, we conclude that the disclination movement observed in real NLCs is first of all a flow property rather than a reorientation process.

3.2. *A nematic with* $\varepsilon_a < 0$

Our second example is to demonstrate the dynamic properties of the nematic using our method. Further, using the dynamic properties we propose another method to generate disclinations. A two dimensional nematic with a negative anisotropic part of the relative dielectric coefficient, ε_a is subjected to an external field in the same direction as the easy axis imposed by the boundary conditions. The field, therefore, causes the nematic to align perpendicular to the z axis, with no preferred direction within the xy plane. Strong anchoring at all of the four boundaries was assumed. To demonstrate the dynamic properties of the system, the simulation was performed in two ways (1) adiabatically, i.e. the time taken for the applied field to reach a maximum value is long compared to the relaxation time of the fluid, and (2) as a non-equilibrium process, which is the reverse case. Both cases were repeatedly simulated with slightly different starting conditions, i.e. with random perturbations of the completely aligned state, without which no Freederickz transition could occur. The perturbation strength was 1 per cent, which means that isotropically distributed random vectors of length 0·01 were added to the initial director field.

The simulation of the first case was done by increasing the applied field in 99 small steps from 0 to 4 times the critical field E_{fred}, cf. equation (8). After each increase up to 1000 iterations were performed to reach an equilibrium state (very close to the Freederickz threshold, even 1000 iterations are not enough to reach equilibrium due to the critical slowing down, cf. [6]). At the field maximum, the director configurations were aligned uniformly in directions which were in any case perpendicular to the applied field, but depend on the different starting conditions.

The simulation of the second case was done by applying the external field quasi-instantaneously. Due to the short time for the field to reach its maximum value (it was increased each third iteration), the director field did not have the chance to align uniformly in any direction within the xy plane. Instead clusters align with different directions separated by defects that were frozen in by the external field.

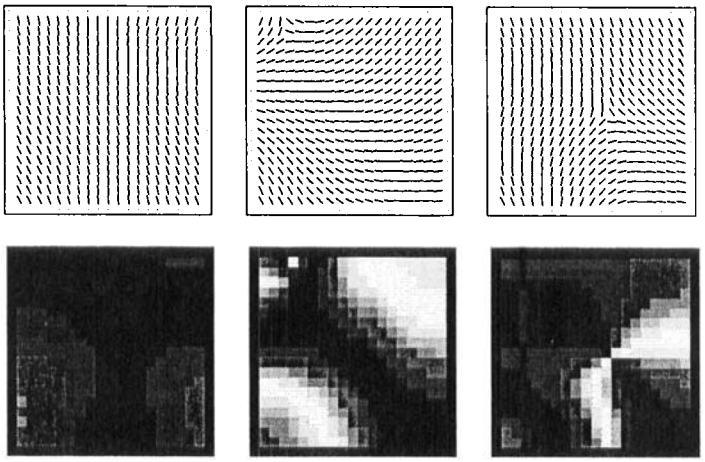

Figure 2. An instantaneously applied external field can, if it is strong enough, preserve the nematic defects in materials with $\varepsilon_a < 0$. Above: different director fields. Below: the same configurations seen under crossed nicols.

Figure 2 shows three director configurations found after 500 iterations, and the corresponding calculated intensities as if watched under crossed analyser and polarizer. (We wish to emphasize that the boundary conditions are not necessary for the occurrence of the disclinations shown in figure 2; since the interior is perpendicular to the wall, the boundary does not affect the components of the director within the plane. Therefore, this part of the simulation could be as well understood as the centre layer of three dimensional nematic with weak anchoring.) The differences are due to the different random perturbations of the initial state. In the absence of the external

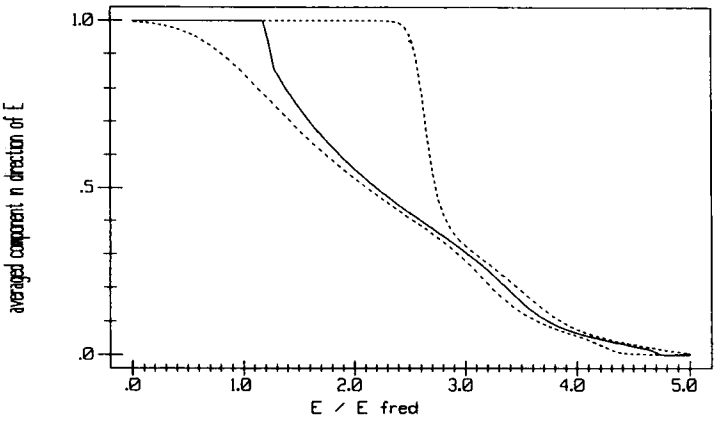

Figure 3. Dynamic properties of the simulation of a nematic with a negative ε_a. The averaged component of the director field reached after iterations plotted versus the field strength exhibits a hysteresis (dashed). Solid: static values.

See his book *Die Lehre von den flüssigen Krystallen und ihre Beziehung zu den Problemen der Biologie*. They indicate that Lehmann already knew about nematic symmetry and the topological shape of nematic defects. he named the specific types of defects displayed here 'half core points' and 'half convergence points', that is disclinations of strength $\pm\frac{1}{2}$ in today's notation. Apparently what he did was much less trivial than the reverse process which we have performed in this paper.

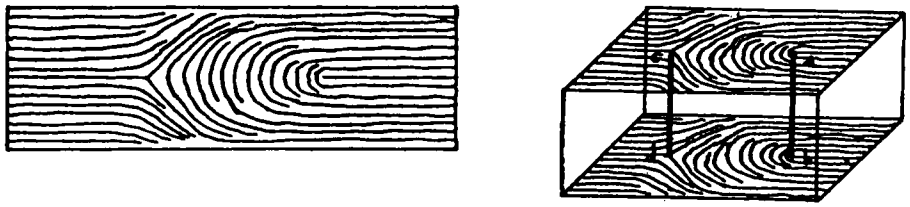

(*a*) (*b*)

Figure 4. As early as 1904, Lehmann deduced the sketches, reproduced here, from his numerous observations of liquid crystals under the polarization microscope. They indicate that Lehmann already knew about the nematic symmetry and the topological shape of nematic defects.

Financial support by the Deutsche Forschungsgemeinschaft via the Sonderforschungsbereich Anisotrope Fluide (SFB 335) is gratefully acknowledged. We thank Professor Dr. W. Muschik, Dipl. Phys. R. Ellinghaus, Dipl. Phys. R. Macdonald, Dipl. Ing. G. Gleske (Technische Universität Berlin), Dipl. Phys. G. Haas (Institut für theoretische Elektrotechnik Karlsruhe) and Professor Dr. R. Hornreich (Weizmann Institute) for helpful discussions. Part of the numerical calculations was performed on the Hewlett-Packard 9000/840 of the Prozessrechner-Verbund-Zentrale of the Technische Universität Berlin. We thank Dr. K. Rebensburg and his staff for their advice.

References

[1] De Gennes, P. G., 1974 *The Physics of Liquid Crystals* (Clarendon Press). Stephen, M. J., and Straley, J. P., 1974 *Rev. mod. Phys.*, **46**, 617.
[2] Kelker, H., and Hatz, R., 1980, *Handbook of Liquid Crystals* (Verlag Chemie).
[3] Vertogen, G., and De Jeu, W. H., 1988, *Thermotropic Liquid Crystals, Fundamentals* (Springer).
[4] Lehmann, O., 1904, *Flüssige Kristalle* (W. Engelmann). Lehmann, O., 1917, *Die Lehre der Flüssigen Kristalle und ihre Beziehung zu den Problemen der Biologie* (Bergmann).
[5] Trebin, H. R., 1982, *Adv. Phys.*, **31**, 195.
[6] Kilian, A., and Hess, S., 1989, *Z. Naturf.* (*a*), **44**, 693.
[7] Hess, S., 1975 *Z. Naturf.* (*a*), **30**, 728, 1224; *Ibid.*, **31**, 1507.
[8] Hess, S., and Pardowitz, I., 1981, *Z. Naturf.* (*a*), **36**, 554.
[9] Hess, S., 1986, *J. non-equilib. Thermodyn.*, **11**, 176.
[10] Hess, S., 1976, *Z. Naturf.* (*a*), **31**, 1034.
[11] Pardowitz, I., and Hess, S., 1982, *J. chem. Phys.*, **76**, 1485.
[12] Baur, G., 1980, *The Physics and Chemistry of Liquid Crystal Devices*, edited by G. Sprokel (Plenum Press), p. 61. Baur, G., 1981, *Molec. Crystals liq. Crystals*, **63**, 45. Berreman, D. W., 1983, *Phil. Trans. R. Soc.* A, **309**, 203.
[13] Bos, P. J., and Koehler, K. R., 1984, *Molec. Crystals liq. Crystals*, **113**, 329.
[14] Heynderickx, I., and Van Spran, H. A., 1989, *Proc. 18. Freiburger Arbeitstagung Flüssigkristalle* (Fraunhofer Institut für Angewandte Festkörperphysik, Freiburg).
[15] Eichler, H. J., and MacDonald, R., 1989, *Proc. 18. Freiburger Arbeitstagung Flüssigkristalle* (Fraunhofer Institut für Angewandte Festkörperphysik, Freiburg).
[16] Kilian, A., and Hess, S., 1990 (to be published).

field these director configurations would not be stable, whereas here they seem to be frozen in.

Figure 3 demonstrates the dynamic properties of the simulation. It exhibits the static and dynamic response of the director field to an external field. The averaged component of the director field in the direction of the applied field **E** was plotted versus the strength of the external field **E** (upper dashed line). Each tenth iteration, the field strength was increased by $0{\cdot}1\,E_{\text{fred}}$, from 0 to $10\,E_{\text{fred}}$. Afterwards, the reverse process was performed (dashed line at bottom). The time corresponding to ten iteration steps is shorter than the relaxation time, especially near the critical field strength E_{crit} (the relaxation time τ_{rel} is proportional to $|E - E_{\text{fred}}|^{-1}$ [6]). Therefore, this is a non-equilibrium process, and a hysteresis appears. The solid line refers to the corresponding adiabatic process, which was done by 1000 iterations after each increase of the applied field.

4. Concluding remarks

An algorithm has been developed which allows the numerical calculation of the dynamic and the static behaviour of the director field, **n**, with the correct nematic symmetry property where **n** and $-\mathbf{n}$ are equivalent. The special case of the one coefficient approximation for the Frank elastic energy has been investigated. The generalization to two different coefficients, in particular the case where $K_1 = K_3 \neq K_2$, is straightforward. For the general case of three different elastic coefficients K_1, K_2, K_3 we have to start from a more complicated equation of the type [11]

$$f_{NN} = A(\partial_\lambda a_{\mu\nu})(\partial_\lambda a_{\mu\nu}) + B(\partial_\nu a_{\nu\mu})(\partial_\lambda a_{\lambda\mu}) + Ca_{\mu\nu}(\partial_\mu a_{\lambda\kappa})(\partial_\nu a_{\lambda\kappa}).$$

Equation (1) corresponds to the choice of $4A = K_1 = K_2 = K_3$, and $B = C = 0$. The extension of the present method to nematics with a spontaneous twist seems to be feasible.

The applications considered here were chosen to indicate the difference between the conventional vectorial algorithm and our tensorial algorithm. Our algorithm is essential for the simulation of the defects typical in nematics, as displayed in figures 1 and 2, and, to give a quantitative analysis of the static and the dynamic response of the local orientation when the system is subject to an external field. Furthermore, the method allows a systematic analysis of the effect of modified boundary conditions, (e.g. caused by scratches, imperfections, and modulations of the anchoring of the molecules of a surface) on the behaviour of a nematic cell.

The method proved reliable in respect of the Frederickz threshold [6] and the orientational dynamic time-scaling [16], at least if flow processes are negligible. As far as disclinations are concerned, however, it yields a more qualitative picture, which may partly be due to the neglected flow. Also, the prediction of the frozen in disclinations shown in figure 2 still lacks experimental confirmation.

In view of the interest for display design [12], the study of the π cell and analogous devices [13] as well as of supertwist cells [14] is desirable. Furthermore, the director field under the influence of a strong laser field, as observed in non-linear optical experiments [15], can be treated. It would be interesting to calculate optical properties from the simulated director field in order to compare with experiment.

5. Historical remark

Here, some historical remarks about the connection between disclinations, nematic symmetry and contrast pictures are made.

As early as 1904, Lehmann [4] deduced the sketches, reproduced here as figure 4, from his numerous observations of liquid crystals under the polarization microscope